Exploiting the Facile Oxidation of Evaporated Gold Films to Drive Electroless Silver Deposition for the Creation of Bimetallic Au/Ag Surfaces

Blake J. Plowman,[a] Matthew R. Field,[b] Suresh K. Bhargava[a] and Anthony P. O'Mullane[b]*

Gold is often considered as an inert material but significantly it has been demonstrated that it possesses unique electronic, optical, catalytic and electrocatalytic properties when in a nanostructured form.[1] For the latter the electrochemical behaviour of gold in aqueous media has been widely studied on a plethora of gold samples including bulk polycrystalline and single crystal electrodes, nanoparticles, evaporated films as well as electrodeposited nanostructures, particles and thin films.[1b, 2] It is now well established that the electrochemical behaviour of gold is not as simple as an extended double layer charging region followed by a monolayer oxide formation/removal process. In fact the so-called double layer region of gold is significantly more complicated and has been investigated with a variety of electrochemical and surface science techniques. Burke and others[3] have demonstrated that significant processes due to the oxidation of low lattice stabilised atoms or clusters of atoms occur in this region at thermally and electrochemically treated electrodes which were confirmed later by Bond[4] to be Faradaic in nature via large amplitude Fourier transformed ac voltammetric experiments. Supporting evidence for the oxidation of gold in the double layer region was provided by Bard[5] who used a surface interrogation mode of scanning electrochemical microscopy to quantify the extent of this process that forms incipient oxides on the surface which was estimated to be as high as 20 % of a monolayer. This correlated with contact electrode resistance measurements,[6] capacitance measurements[7] and also electroreflection techniques.[8]

It has also been demonstrated that the electrochemical pretreatment of a gold surface significantly impacts on the formation of SAM layers whereby readily oxidised gold is detrimental to the formation of well packed layers.[9] Freshly prepared gold surfaces also appear to be in a metastable state as evidenced by recent studies on the ageing effect of gold nanoparticles and surfaces on electrocatalytic processes.[3d, 10] It was postulated that the initially formed metastable states responsible for high electrocatalytic activity slowly re-arrange into a structurally more stable form that is less active for electrocatalytic processes. Therefore there is a significant amount of evidence that applicable gold materials such as thin films, bulk polycrystalline electrodes and nanoparticles possess an inherent property whereby they can be readily oxidised, in particular at potentials well below that of bulk gold oxide formation at 1.36 V vs SHE as determined by Pourbaix.[11]

Recently galvanic replacement has been demonstrated to be a viable technique for the creation of bimetallic materials. This technique is based upon the reaction of a metallic template in contact with a metallic salt solution, resulting in the replacement of the initial template structure with the secondary metal.[12] The driving force for such galvanic replacement reactions is provided by the difference in the standard reduction potentials of the metal/metal ion couples, and so the use of readily oxidisable templates such as iron, copper or silver has been widely reported. A significant amount of research has been performed using this method, however the galvanic replacement of more noble metals is problematic given the limited number of metals which can be used to replace them. This limitation is highlighted in the case of gold, where the high standard reduction potential for the Au/Au^{3+} couple (1.50 V vs SHE) prohibits galvanic replacement from a thermodynamic viewpoint. However in light of previous work where it was found that nanostructured gold can in fact be readily oxidised at potentials less than 1 V vs SHE this suggests that advantage can be taken of this phenomenon to drive the reduction of metal salts to their metallic form with a lower standard reduction potential such as silver on to the surface of gold.

In this work we investigate in detail the decoration of evaporated gold films with silver, in the absence of an applied potential, as a means to further study the phenomenon of gold oxidation within the double layer region assumed to be due to the presence of surface defects. It should be noted that the electrodeposition of silver on gold has been widely reported, particularly in the case of underpotential deposition of silver on polycrystalline and single crystal gold surfaces.[13] Interestingly however, it was observed in certain cases that silver deposition occurred in the absence of an applied potential but a thorough mechanistic understanding of this process is yet to emerge.[14] Also Wu[15] reported the decoration of thiolate capped gold nanoparticles less than 3 nm in diameter with silver, however the role of the capping agent was unclear.

Evaporated gold was chosen as this is a practical material that is utilised in a wide range of applications and therefore the behaviour of defects on these surfaces may have many implications for its use in electrochemical based sensing, electronics or as a coating material. In addition, FT-ac studies have revealed that these thin gold films demonstrate significant

[a]   B. J. Plowman, Prof. S. K. Bhargava,
       Centre for Advanced Materials and Industrial Chemistry
       School of Applied Sciences
       RMIT University
       GPO Box 2476V, VIC, 3001, Australia
[b]   Dr. A. P. O'Mullane, Dr. M. R. Field
       School of Applied Sciences
       RMIT University
       GPO Box 2476V, VIC, 3001, Australia
       E-mail: anthony.omullane@rmit.edu.au

and stable premonolayer oxidation responses under alkaline conditions (Figure 1) even without activation treatments, thus making them promising candidates for decoration with other metals. It should be noted that these types of responses are also observable under acidic conditions but due to the proposed nature of the oxidation product, i.e. a hydrous oxide, the responses are lower in magnitude.[4] However from Figure 1 it is clear from the higher harmonics, and the 4th harmonic in particular where the contribution from capacitive current is minimal, that there are many Faradaic responses in the double layer region from -0.80 to 0.20 V prior to the onset of bulk oxide formation at 0.20 V. Silver was chosen as a decorating metal, as the standard reduction potential for Ag^+/Ag (0.799 vs SHE) is far removed from that of the Au^{3+}/Au couple (1.50 V vs SHE) and therefore its reduction at a gold surface should be thermodynamically forbidden. The electrocatalytic activity of silver is also distinctly different to that of gold, in particular under acidic conditions where in general it is considered as a poorer electrocatalyst. Therefore the electrocatalytic performance of the Au/Ag material should indicate clearly whether gold defect sites are indeed utilised in the formation process.
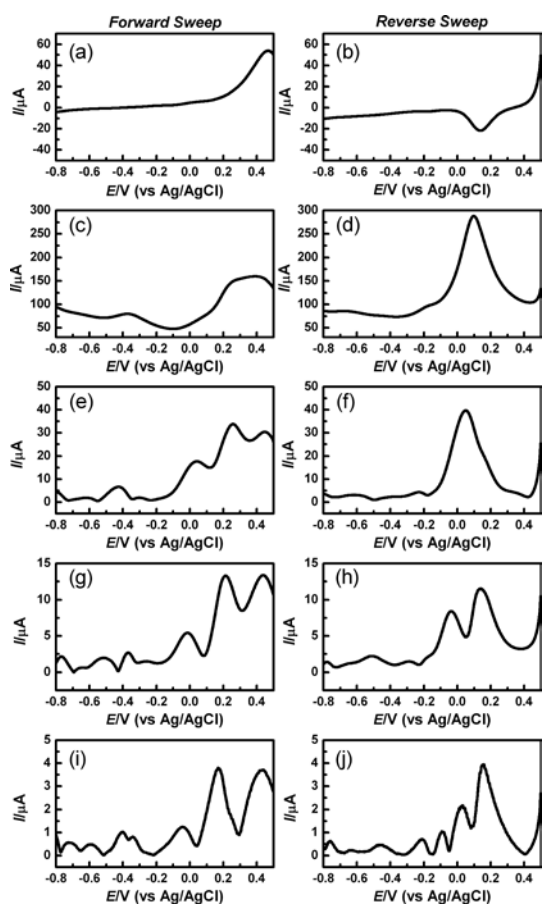

Figure 1. Fourier transformed ac voltammetry recorded at a gold film in 1 M NaOH showing the forward (a-i) and reverse (b-j) scans for the DC (a-b) and first (c-d) to fourth (i-j) harmonic responses. The data was recorded at a sweep rate of 63.33 mV s⁻¹ with an applied sinusoidal perturbation of 100 mV at a frequency of 21.1 Hz.

The decoration of evaporated gold was performed by immersing a thin gold film (150 nm) in a nitrogen-purged solution of 1 mM $AgNO_3$ for five minutes at open circuit potential, following which the films were thoroughly washed with Milli-Q water and allowed to dry. The presence of metallic silver was confirmed by X-ray photoelectron spectroscopy (XPS) (Figure 2), with peaks at 368.6 eV and 374.6 eV corresponding to the $3d_{5/2}$ and $3d_{3/2}$ energy levels of metallic silver.[16] Importantly, no traces of Ag^+ or N species could be detected on the decorated films, showing that the simple washing step was all that was required to remove any weakly adsorbed $AgNO_3$ species from the surface which could alter the subsequent characterisation and performance of the films. It should also be noted that inductively coupled plasma mass spectrometry (ICP-MS) did not detect the dissolution of gold into the decoration solution, in agreement with work by Yang and co-workers on the interaction of hydroxyl radicals with gold surfaces,[17] however the possibility that this occurred below the detection limit of the instrument cannot be discounted. This may also indicate that the oxidation of gold results in the formation of an oxide on the surface.
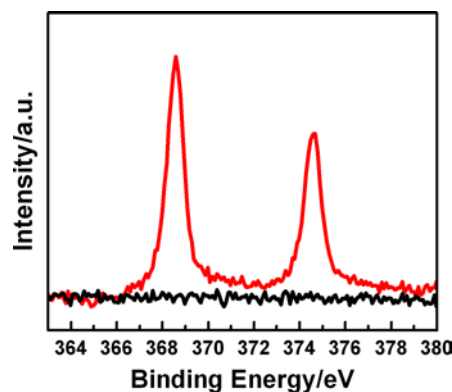

Figure 2. Ag 3d XPS spectra for an evaporated gold film with (red) and without (black) silver decoration.

The electrochemical behaviour of the silver-decorated gold films was tested in 1 M H_2SO_4 (Figure 3), where additional anodic processes were detected after silver decoration (red curve). While the peak potential for this new process is found at 0.89 V (vs Ag/AgCl), a shoulder towards less positive potentials can also be seen with an onset potential of approximately 0.68 V. The occurrence of such features is consistent with previous studies on silver oxidation,[18] which were attributed to factors such as size effects for nanoparticles less than 40 nm in diameter and also to surface coverage and the role of overlapping diffusion layers of the individual particles. It can also be seen from Figure 3 that the charge required to reduce the gold monolayer oxide (peak at ca. 0.93 V) is very similar for both the silver-decorated gold substrate and the unmodified gold substrate. In the former case Ag has been electrochemically stripped from the surface on the forward sweep and therefore this suggests that very little gold is utilised or dissolved in forming silver at the surface which is consistent with the ICP-MS measurements. This data also demonstrates that the surface area of the material is not significantly altered after the decoration process. Similar results were also found for CV studies in 1 M NaOH (Figure S1) which does not result in silver stripping from the surface, where the oxide reduction process for both the Au and Au/Ag samples were comparable in magnitude.
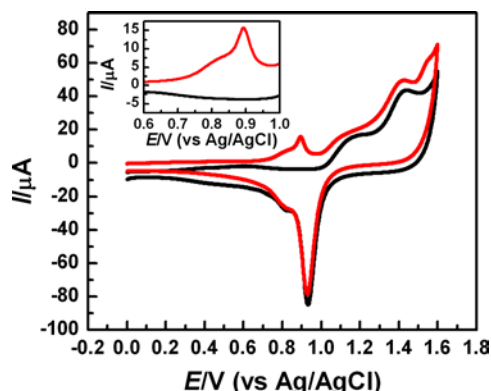
Figure 3: Cyclic voltammetry recorded at 100 mV s⁻¹ in 1 M H_2SO_4 for a gold film (black) and a silver-decorated gold film (red) showing the full scan (a) and an enlarged section showing the oxidation of silver (b).

From the work of Scholz it was found that the selective knockout of gold active sites was achieved through hydroxyl radical attack on surface asperities.[19] By probing inner sphere reactions such as hydrogen evolution and the benzoquinone/hydroquinone couple and comparing these results with the outer sphere $Ru^{3+/2+}$ hexamine couple the participation of active sites was inferred. Here the reactivity towards an outer sphere reaction was probed using ferrocenemethanol (Figure 4a). As can be seen no significant differences could be observed between the voltammograms recorded at the Au and Au/Ag films which is expected as this is a surface insensitive process governed by planar diffusion. In comparison the hydrogen evolution reaction (HER) was investigated as an inner sphere reaction as it is significantly more facile at polycrystalline gold compared to polycrystalline silver under acidic conditions.[20]
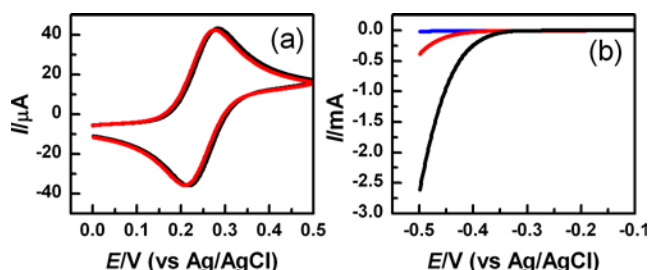

Figure 4. Cyclic voltammetry of a gold film (black), a silver decorated film (red) and a silver film (blue) recorded in a solution of 1 mM ferrocenemethanol in 0.1 M KNO_3 (a) and 1 M H_2SO_4 (b). Sweep rates were 100 mV s⁻¹ for (a) and 5 mV s⁻¹ for (b).

In Figure 4b the HER shows a shift in the onset potential of approximately 60 mV towards more negative potential values along with a substantial decrease in current magnitude after decorating the gold film with silver. While the exposed gold on this surface still shows greater activity towards the HER than a silver film, this shutting down of electrocatalytic activity is highly significant as the electrochemically active surface area of the electrode does not change significantly (Figure S1). This indicates that the gold defect sites that were responsible for the spontaneous reduction of Ag⁺ are almost solely responsible for the electrocatalytic activity of the gold film towards HER. From calculating the charge involved in stripping silver from the surface in H_2SO_4[13a] a surface area of X cm² was determined. The electrochemically active surface area of the gold surface

was determined by the charge required to reduce the monolayer oxide,[21] which gave a value of X cm² which equates to a roughness factor of X. If we assume the transfer of 3 electrons from the oxidation of gold then this implies 7% of the gold surface was involved in the defect driven oxidation process.

In order to observe the nature of the silver deposit on the gold surface, scanning electron microscopy (SEM) was performed (Figure S2), however the morphology of the silver deposit could not be observed, which was assumed to be due to the working resolution limit of the instrument. This is in contrast to discrete nanoparticles of silver that are spontaneously formed on highly porous electrodeposited gold films which contain a significant number of defect sites.[22] It must also be stressed that these Au films are not electrochemically pre-treated prior to decoration as seen previously for the modification of platinum electrodes with gold or nanoporous gold with platinum that had been deliberately activated via cathodic polarisation.[23] While transmission electron microscopy (TEM) can offer enhanced resolution, the difficulty involved in preparing these films for TEM while preserving their integrity precluded the analysis of the evaporated gold films on Si substrates as studied here. An alternative substrate was provided by utilising a commercially available gold TEM grid with a single crystal gold film. It should be noted that although the film was nominally single crystal gold in a (100) orientation many defects were found to be present on the surface, such as raised steps (Figure 5a). After performing the decoration process as outlined for the gold substrates, the presence of silver on the gold film could be observed by both energy dispersive X-ray spectroscopy (EDX) (Figure S3) and XPS (Figure S4) of the decorated TEM grid. Additionally, by use of EDX mapping the distribution of silver across the TEM grid could be determined (Figure 5b), which shows a sparse but relatively even coverage across the surface which is in agreement with the type of loading estimated by CV experiments. High resolution imaging was then performed on regions showing higher silver coverage, and as can be seen from the representative image in Figure 5c discrete nanoparticles of Ag could not be observed, indicating that the decoration of silver on the gold TEM grid occurred as a sub-monolayer deposit. While these results do not directly correlate to the evaporated polycrystalline films, they are in agreement with the finding that the growth of the silver deposits does not result in the formation of structures large enough to be imaged by SEM (approx. 10 nm).

While the simple protocol discussed above was found to be suitable for the spontaneous reduction of silver, other variables that may influence the decoration process were also investigated. In particular the photoreduction of $AgNO_3$ was considered, however it was found that after repeating the decoration process under dark conditions that similar voltammetric profiles to that in Figure 3 could be obtained. The presence of O_2 was also investigated to see if it influenced the chemical oxidation of defect sites and thereby reduced the extent of silver decoration on the surface. This was not found to be the case, as gold films decorated in an O_2-saturated solution of 1 mM $AgNO_3$ again produced similar CVs in 1 M H_2SO_4 to samples decorated in N_2-purged solutions.
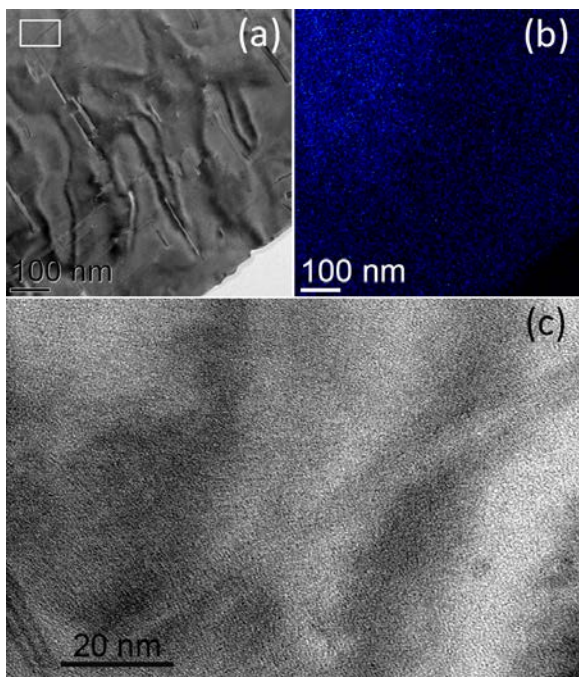
Figure 5. High resolution TEM (HRTEM) image of a silver-decorated single crystal gold TEM grid (a) and the corresponding EDX map (b) showing the distribution of silver (blue) across the surface. A representative high magnification image is presented in (c), relating to the region in (a) indicated by the white rectangle.

It is clear from the HER data that gold defect sites are selectively utilised in the creation of the Ag/Au surface which significantly decreases the electrocatalytic activity of the bimetallic surface for this reaction. However it is also important to note that the electrocatalytic activity of a material is highly correlated to the specific reaction of interest as the result of a contribution of numerous factors including how the reactants adsorb, react and desorb from the surface and indeed the nature of the defect site present on the surface. This can in turn be influenced by the composition, size, shape, crystallographic orientation and porosity of the material, and therefore different materials are better suited to particular electrocatalytic reactions than others. The use of bimetallic electrodes can also offer benefits over their single metallic counterparts through synergistic effects between the two metals where the cases of Pt/Au and Pt/Ru in particular are well known for fuel cell relevant electrocatalytic reactions.[24] In this work, while the HER was found to be substantially decreased at the silver decorated film, improved electrocatalytic responses could be observed for the reduction of oxygen under acidic conditions (Figure 6a). This is an important electrocatalytic reaction, studied both as a model system and of interest for fuel cells, where the sluggish reduction of oxygen can often be a limiting factor.[25] This is indeed the case at the evaporated gold film where a well-defined reduction peak could not be observed (Figure 6a). However for the silver-decorated gold film there is a significant shift in the onset potential of ca. 170 mV compared to the unmodified gold film. This is opposite to the HER case and also the work of Scholz who demonstrated that gold treated with Fenton's reagent severely impeded the oxygen reduction reaction. It seems here that although gold defect sites have

been decorated with silver the resulting bimetallic surface is quite active for oxygen reduction. This is not likely to be due to electronic effects as the XPS results indicated that the binding energy for gold is not significantly altered by the presence of silver.
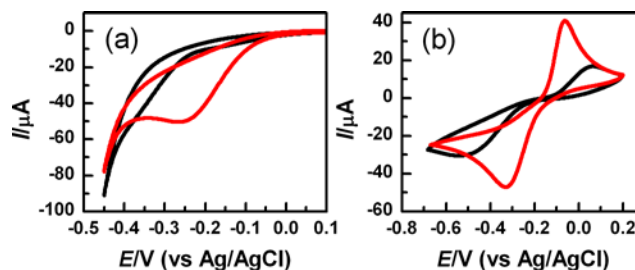

Figure 6. Electrocatalytic activity of a gold film (black) and a silver-decorated gold film (red) demonstrated by CV in O_2 saturated 1 M H_2SO_4 (a) and 1 M NaOH (b) at 50 mV s^{-1}.

The electrocatalytic reduction of oxygen was also carried out in 1 M NaOH (Figure 6b) which is generally the more studied system. The voltammetry at the gold substrate again appears quite sluggish, with evidence of the process being quasi-reversible. Rotating ring-disk electrode (RRDE) studies (Figure 7) carried out on a commercially available polycrystalline gold disk electrode (BAS) indicate the formation of hydrogen peroxide during the reduction sweep and suggests that this is the reason for the observed quasi-reversibility. Upon decoration of the evaporated gold film with silver (Figure 6b) the voltammetry is considerably altered, showing a shift in the reduction peak of approximately 200 mV towards more positive potentials as compared to the gold film. The process is also more reversible with a peak-to-peak separation of 270 mV compared to 610 mV for evaporated gold and indicates promotion of the two-electron pathway for oxygen reduction to hydrogen peroxide, which was also confirmed by RRDE studies on a silver-decorated gold disk (Figure 7). Therefore under acidic and alkaline conditions the presence of silver is beneficial for the oxygen reduction reaction.
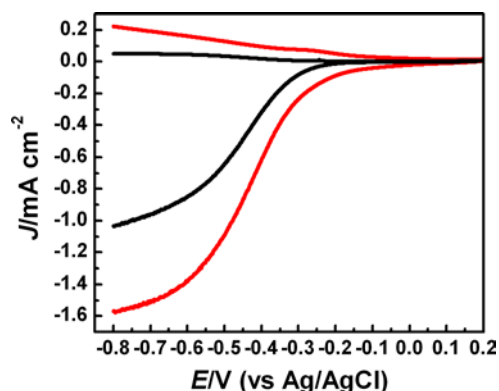

Figure 7: Rotating ring disk electrode studies showing a gold disk (black) and silver-decorated gold disk (red) electrode in an O_2 saturated 1 M NaOH solution. The platinum ring electrode was held at 0.3 V (vs Ag/AgCl) in order to detect peroxide formation on the disk, with the results normalised for the geometric areas of the electrodes. The electrode rotation rate was 2000 RPM and the sweep rate was 10 mV s^{-1}.

It is known that the electrochemical behaviour of defect sites on gold is quite varied and are oxidised over a wide range of potentials in the double layer region as well as the premonolayer responses exhibiting super-Nernstian pH shifts.[26] Therefore the coverage of sites that may be responsible for the deactivation of gold for HER may not in fact participate in oxygen reduction. It should also be noted that this reaction is somewhat controversial at silver where discrepancies exist between the effect of size and crystallographic nature of silver regarding the two- or four-electron pathways at different pH values.[27] Given that we do not have clear evidence for the size of silver deposited on the surface and are assuming sub-monolayer coverage the exact influence of silver in our system will need further investigation.

In summary we have demonstrated that defect sites exist on evaporated gold films and can be used to facilitate the reduction of Ag^+ to metallic Ag even though the reaction is thermodynamically forbidden at bulk gold. The resulting coverage of defect sites does not affect the overall surface area of the electrode or result in detectable gold dissolution and from TEM imaging suggests that complete surface coverage is not achieved but rather sub-monolayer coverage. The selective decoration of gold defect sites with Ag severely inhibits the HER even though the majority of the gold surface is still available for the reaction. However, for the oxygen reduction reaction under acidic or alkaline conditions silver decoration has a beneficial effect in enhancing electrocatalytic performance. This approach highlights that gold surfaces, which have not been activated by chemical, sonochemical or electrochemical methods, are indeed inherently rich in defect sites and that this behaviour needs to be considered when using gold in various applications. Given that the evaporated gold film is still rough on the nanoscale with a roughness factor of X, the next stage of investigation is at single crystal surfaces or ultra-flat films to further elucidate the reaction mechanism. However, this method of decorating gold surfaces is expected to be applicable to a wide range of other metals and may open up a way of investigating the participation of selective defect sites that are involved in electrocatalytic reactions at surfaces of various defect levels.

Experimental Section

The gold and silver films employed in this study were prepared by e-beam evaporation (Balzers™ electron beam evaporator) of a 10 nm Ti adhesion layer on a silicon (100) substrate (Montco Silicon Technologies) followed by 150 nm of Au or Ag. Prior to use the films were cleaned by successive immersions in acetone (Chem-Supply), methanol (Merck) and Milli-Q water (18.2 MΩ cm) for five minutes each, and then dried under a stream of nitrogen. To obtain comparable geometric areas the films were then masked using Kapton tape. This gave a geometric area of X cme, the electrochemically active surface area was found to be Y cm2. Decoration with silver was performed at open circuit potential by immersing the films in a solution of $AgNO_3$ (Merck) for a specified time. Prior to immersion these solutions were degassed by bubbling with high purity nitrogen for at least five minutes unless specified. After immersion the substrates were thoroughly washed in two successive containers of Milli-Q water in order to remove any weakly adsorbed species. Electrochemical properties were studied using a CH Instruments electrochemical analyser (CHI 760C) using a three-electrode configuration with a Ag/AgCl

reference electrode and a graphite counter electrode. All electrode potentials are quoted against the Ag/AgCl reference. Solutions were made using ferrocenemethanol (Aldrich), NaOH (Merck), H_2SO_4 and KNO_3 (Ajax) as received. All solutions used for electrochemical testing were degassed by bubbling nitrogen for at least five minutes, except in the case of oxygen reduction experiments which were bubbled with high purity oxygen (5.0 Coregas) for at least fifteen minutes prior to experiments. Rotating ring disk electrode studies used a gold disk and platinum ring configuration and was polished using a 0.05 μm alumina slurry, cleaned with ultrasonication and rinsed with Milli-Q water prior to use. Inductively coupled plasma mass spectrometry was performed using an Agilent 7700x instrument with an ASX-520 autosampler. Electron microscopy was performed using an FEI Nova SEM instrument (Nova 200) equipped with EDX as well as a JEOL 2100 TEM with a FEG source. XPS was performed using a Thermo K-Alpha instrument at a pressure better than 10-9 Torr, with the data being referenced to the adventitious C 1s binding energy of 285 eV.

[1]   a) M. Haruta, T. Kobayashi, *Chem. Lett.* **1987**, *16*, 405-408; b) M. C. Daniel, D. Astruc, *Chem. Rev.* **2004**, *104*, 293-346.

[2]   a) A. Hamelin, *J. Electroanal. Chem.* **1996**, *407*, 1-11; b) A. Hamelin, A. M. Martins, *J. Electroanal. Chem.* **1996**, *407*, 13-21; c) A. Sarapuu, K. Tammeveski, T. T. Tenno, V. Sammelselg, K. Kontturi, D. J. Schiffrin, *Electrochem. Commun.* **2001**, *3*, 446-450; d) A. P. O'Mullane, S. J. Ippolito, Y. M. Sabri, V. Bansal, S. K. Bhargava, *Langmuir* **2009**, *25*, 3845-3852; e) C. L. Perdriel, A. J. Arvia, M. Ipohorski, *J. Electroanal. Chem.* **1986**, *215*, 317-329.

[3]   a) L. D. Burke, A. P. O'Mullane, *J. Solid State Electrochem.* **2000**, *4*, 285-297; b) L. D. Burke, A. J. Ahern, A. P. O'Mullane, *Gold Bull.* **2002**, *35*, 3-10; c) L. D. Burke, A. M. O'Connell, A. P. O'Mullane, *J. Appl. Electrochem.* **2003**, *33*, 1125-1135; d) G. Dutta, K. Jo, H. Lee, B. Kim, H. Y. Woo, H. Yang, *J. Electroanal. Chem.* **2012**, *675*, 41-46; e) D. Kotnik, M. Novič, W. R. LaCourse, B. Pihlar, *J. Electroanal. Chem.* **2011**, *663*, 30-35.

[4]   B. Lertanantawong, A. P. O'Mullane, W. Surareungchai, M. Somasundrum, L. D. Burke, A. M. Bond, *Langmuir* **2008**, *24*, 2856-2868.

[5]   J. Rodríguez-López, M. A. Alpuche-Avilés, A. J. Bard, *J. Am. Chem. Soc.* **2008**, *130*, 16985-16995.

[6]   V. A. Marichev, *Russ. J. Electrochem.* **1999**, *35*, 434-440.

[7]   G. M. Schmid, R. N. O'Brien, *J. Electrochem. Soc.* **1964**, *111*, 832-837.

[8]   G. Nguyen Van Huong, C. Hinnen, J. Lecoeur, *J. Electroanal. Chem.* **1980**, *106*, 185-191.

[9]   R. F. Carvalhal, R. Sanches Freire, L. T. Kubota, *Electroanalysis* **2005**, *17*, 1251-1259.

[10]   H. J. Kang, S. Patra, J. Das, A. Aziz, J. Jo, H. Yang, *Electrochem. Commun.* **2010**, *12*, 1245-1248.

[11]   M. Pourbaix, *Atlas of Electrochemical Equilibria in Aqueous Solution*, Pergamon, Oxford, **1966**.

[12]   a) C. M. Cobley, Y. Xia, *Mater. Sci. Eng. R* **2010**, *70*, 44-62; b) Y. Yin, C. Erdonmez, S. Aloni, A. P. Alivisatos, *J. Am. Chem. Soc.* **2006**, *128*, 12671-12673; c) A. Pearson, A. P. O'Mullane, V. Bansal, S. K. Bhargava, *Chem. Commun.* **2010**, *46*, 731-733.

[13]   a) V. Rooryck, F. Reniers, C. Buess-Herman, G. A. Attard, X. Yang, *J. Electroanal. Chem.* **2000**, *482*, 93-101; b) S. B. Aoun, Z. Dursun, T. Koga, G. S. Bang, T. Sotomura, I. Taniguchi, *J. Electroanal. Chem.* **2004**, *567*, 175-183; c) S. Garcia, D. Salinas, C. Mayer, E. Schmidt, G. Staikov, W. J. Lorenz, *Electrochim. Acta* **1998**, *43*, 3007-3019; d) M. C. Santos, L. H. Mascaro, S. A. S. Machado, *Electrochim. Acta* **1998**, *43*, 2263-2272.

[14]   P. Mrozek, Y.-E. Sung, A. Wieckowski, *Surf. Sci.* **1995**, *335*, 44-51.

[15]   Z. Wu, *Angew. Chem. Int. Edit.* **2012**, *51*, 2934-2938.

[16]   a) F. M. Cuevas-Muñiz, M. Guerra-Balcázar, F. Castaneda, J. Ledesma-García, L. G. Arriaga, *J. Power Sources* **2011**, *196*, 5853-5857; b) S. Prathap Chandran, J. Ghatak, P. V. Satyam, M. Sastry, *J. Colloid Interface Sci.* **2007**, *312*, 498-505.

[17]   K. Jo, G. Dutta, J. W. Kim, H. Yang, *Chem. Commun.* **2012**, *48*, 8841-8843.

[18]   a) O. S. Ivanova, F. P. Zamborini, *J. Am. Chem. Soc.* **2010**, *132*, 70-72; b) M. Giovanni, M. Pumera, *Electroanalysis* **2012**, *24*, 615-617; c)

S. E. Ward, F. W. Campbell, R. Baron, L. Xiao, R. G. Compton, *J. Phys. Chem. C* **2008**, *112*, 17820-17827.

[19]   A. Nowicka, U. Hasse, M. Hermes, F. Scholz, *Angew. Chem. Int. Edit.* **2010**, *49*, 1061-1063.

[20]   J. Greeley, T. F. Jaramillo, J. Bonde, I. B. Chorkendorff, J. K. Norskov, *Nature Mater.* **2006**, *5*, 909-913.

[21]   S. Trasatti, O. A. Petrii, *Pure Appl. Chem.* **1991**, *63*, 711-734.

[22]   B. J. Plowman, A. P. O'Mullane, S. K. Bhargava, *Faraday Discuss.* **2011**, *152*, 43-62.

[23]   a) A. P. O'Mullane, S. K. Bhargava, *Electrochem. Commun.* **2011**, *13*, 852-855; b) S. Cherevko, N. Kulyk, C.-H. Chung, *Electrochim. Acta* **2012**, *69*, 190-196.

[24]   a) J. Liu, L. Cao, W. Huang, Z. Li, *ACS Appl. Mater. Interfaces* **2011**, *3*, 3552-3558; b) X. Han, D. Wang, D. Liu, J. Huang, T. You, *J. Colloid Interface Sci.* **2012**, *367*, 342-347; c) H. Liu, C. Song, L. Zhang, J. Zhang, H. Wang, D. P. Wilkinson, *J. Power Sources* **2006**, *155*, 95-110.

[25]   C. J. Zhong, J. Luo, B. Fang, B. N. Wanjala, P. N. Njoki, R. Loukrakpam, J. Yin, *Nanotechnology* **2010**, *21*, 062001.

[26]   L. D. Burke, M. E. G. Lyons, in *Modern Aspects of Electrochemistry, Vol. 18* (Eds.: R. E. White, J. O. M. Bockris, B. E. Conway), Plenum Press, New York, **1986**, pp. 169-248.

[27]   a) M. Chatenet, L. Genies-Bultel, M. Aurousseau, R. Durand, F. Andolfatto, *J. Appl. Electrochem.* **2002**, *32*, 1131-1140; b) J. S. Spendelow, A. Wieckowski, *Phys. Chem. Chem. Phys.* **2007**, *9*, 2654-2675.

A golden approach for the formation of bimetallic (electro)catalysts: The facile synthesis of gold-silver bimetallic surfaces was investigated through the spontaneous decoration of silver on evaporated gold films. This spontaneous reaction was found to be driven by the oxidation of the gold surfaces at potentials lower than that expected for bulk gold, providing a simple method of metal decoration to create bimetallic surfaces.

Spontaneous Decoration

Gold Active Site
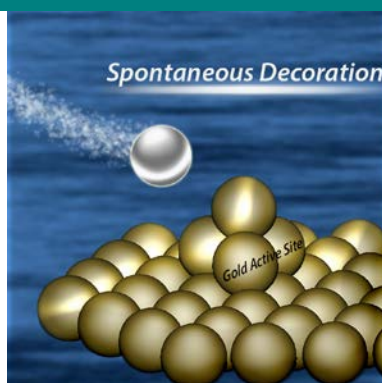
Blake J. Plowman, Matthew R. Field, Suresh K. Bhargava, Anthony P. O'Mullane*

Exploiting the facile oxidation of evaporated gold films to drive electroless silver deposition for the creation of bimetallic Au/Ag surfaces
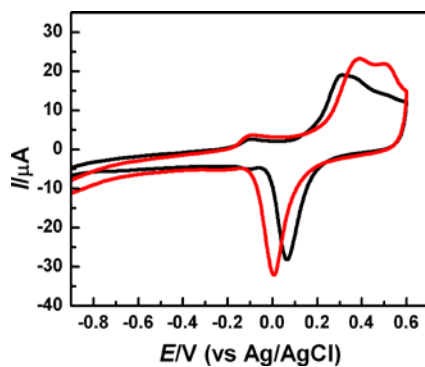
Figure S1: Cyclic voltammetry recorded at 50 mV s^{-1} in 1 M NaOH for a gold film (black) and a silver-decorated gold film (red).
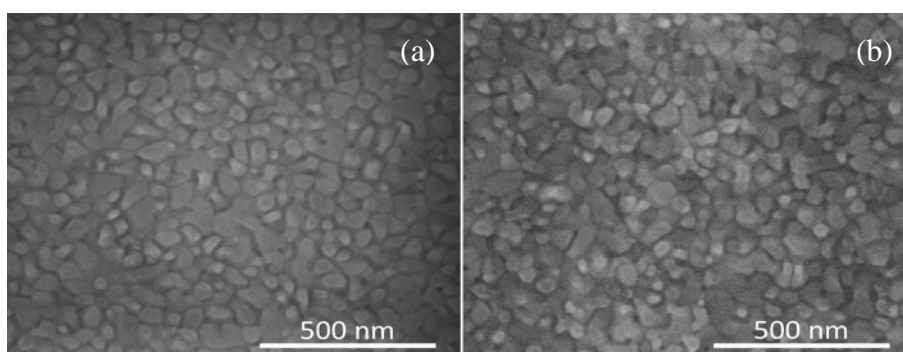

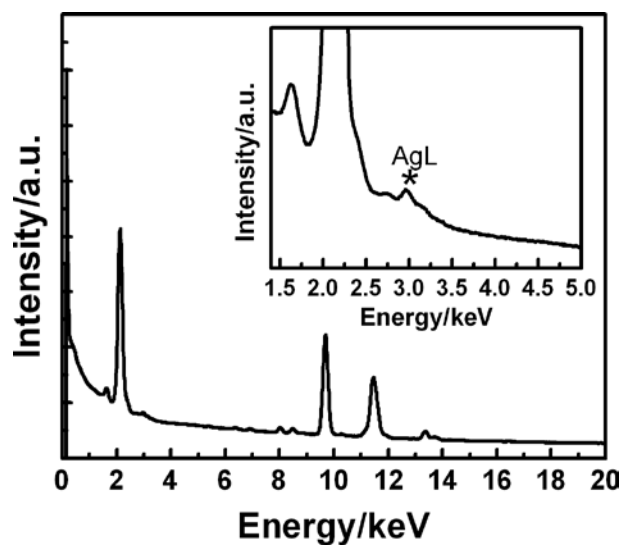**Figure S2.** SEM images of evaporated gold films before (a) and after (b) silver decoration.
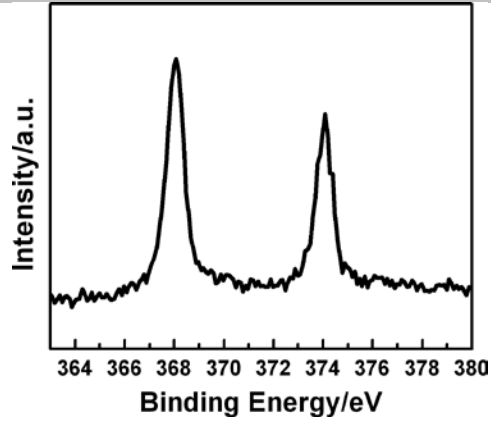

Figure S3. EDX spectrum of a silver-decorated gold TEM grid.

Figure S4. Ag 3d XPS spectra for a silver-decorated TEM grid.